A model for current sheets and reconnection in X-ray bright points

D. W. Longcope
Department of Physics, Montana State University
Bozeman, MT 59717

ABSTRACT

X-ray bright points are believed to result from the interaction of two small magnetic features of opposite polarity. As these features move apart, flux interconnecting them can become disconnected and joined to overlying magnetic field. For features moving toward one another this process will occur in reverse. In either case this magnetic reconnection occurs at the separator field line (Parnell, Priest and Golub 1994). Assuming that reconnection can occur only after it is "triggered" the process will heat the plasma nearby the separator, thereby giving rise to the x-ray brightening. This can be quantitatified using a recent model of current sheet formation and reconnection along separators (Longcope 1996). Application of this model predicts the heating from reconnection based on the observable magnetic quantities of flux, field strength and polar separation. In addition the model predicts morphological aspects of the bright points such as the apparent angle between the axes of the x-ray loop and the magnetic bipole (Kankelborg et al. 1996).

1. Introduction

X-ray bright points (XBPs) are small ($\lesssim 60''$) isolated point-like or loop-like features found most often in coronal holes and quiet sun regions. Originally observed in soft X-ray images (Golub et al. 1974), they are also observed in radio (Habbal et al. 1986) and EUV line emission (Kankelborg et al. 1996). It has been shown that the locations of XBPs correlate strongly with the locations of pairs of opposing magnetic elements, called *bipoles*, found in magnetograms (Golub et al. 1977, Kankelborg et al. 1996, Falconer, Moore, & Porter 1997). This has lead to the hypothesis that XBPs result from some form of interaction between opposing magnetic poles.

Typical XBPs are loops ~ 20 Mm (30 arc sec) long which last for life-times ranging from 2 hours to 48 hours. In a survey of Skylab S-054 data the average life-time was determined to be 8 hours (Golub et al. 1974). The X-ray luminosity can fluctuate over time scales as short as $\sim$ 10 minutes (Nolte, Solodyna, & Gerassimenko 1979, Habbal, Dowdy, & Withbroe 1990, Strong et al. 1992, Harvey et al. 1994b). In addition to the power radiated in X-rays and EUV, models suggest that the coronal plasma also loses power by thermal conduction into the relatively cooler chromosphere (Habbal, Dowdy, & Withbroe 1990, Kankelborg et al. 1996, Kankelborg, Walker, & Hoover 1997). These observed and inferred losses must be balanced by a source of energy (heating) to keep the XBP bright over its life-time (Nolte, Solodyna, & Gerassimenko 1979, Kankelborg et al. 1996). Observed variability indicates that this heating source is at least partly impulsive (Nolte, Solodyna, & Gerassimenko 1979, Habbal, Dowdy, & Withbroe 1990). Kankelborg et al. (1997) applied a steady-state energy-balance model to 23 XBPs observed with a rocket-born FUV instrument on May 13, 1991. The model can be used to infer the total heating power required by each XBP. Computed power requirements range from 4×10^{22} to 4×10^{24} ergs/sec in the sample of 23 XBPs; the median value is 10^{24} erg/sec.

It has been proposed that the heating source for XBPs is magnetic reconnection occurring between the poles. This hypothesis would explain the observational fact, confirmed in every study, that whenever an XBP is found there is *almost always* a magnetic bipole in the immediate vicinity. This association has been shown to be far stronger than pure chance might produce (Falconer, Moore, & Porter 1997). It is equally important to note, however, that many magnetic bipoles (perhaps more than half of them) are *not* associated with XBPs (Harvey et al. 1994a).

There has been some disagreement over the type of bipoles with which XBPs are most frequently associated. Golub et al. (1977) found a majority of XBPs associated with separating (emerging) bipoles, also called ephemeral active regions. A more recent statistical study (Webb et al. 1993) reports an overwhelming 88% of XBPs associated with converging (canceling) bipoles. In neither case is the time variation in the X-ray emission related simply to any event in the magnetic field, nor does the emission accompany the actual appearance or disappearance of the poles (Harvey et al. 1994a). Instead the fluctuating emission occurs above two poles which are gradually approaching one another, separating from one another, or simply passing near one another (Harvey et al. 1994b).

If the reconnection hypothesis is correct then XBPs may offer the simplest case of magnetic reconnection in the solar corona. In a typical example two magnetic poles of opposing polarity, each with flux $\psi \sim 10^{19}$ Mx, interact with one another. Most theories of the coronal magnetic field suggest that a large-scale overlying field would be present as well, and might affect the reconnection process (Heyvarts, Priest, & Rust 1977). Any model for reconnection in this context should answer two basic questions: how close must poles approach before interacting? and how much heating energy does the process of magnetic reconnection generate?

Several theoretical models of XBPs resulting from magnetic reconnection have been proposed. These models address the interaction distance and heating power issues to varying degrees. Priest, Parnell and Martin (1994) presented a two dimensional model (the converging flux model) of interacting magnetic poles (sheets) in which an estimate of the reconnection energy is found. Since it is strictly two-dimensional, however, its morphology cannot be compared to observations. Furthermore, its interaction distance scales differently than expected in three-dimensions.

Three-dimensional models for reconnection have also been developed (Parnell, Priest, & Golub 1994, Mandrini et al. 1996). Parnell et al. employ a magnetic charge topology model (Baum & Bratenahl 1980, Gorbachev & Somov 1988) where reconnection occurs at the *separator* field line. Mandrini et al. use a closely related model with continuous magnetic field; in it the reconnection occurs along a quasi-separatrix layer (Longcope & Strauss 1994, Priest & Démoulin 1995). These models agree well with observed morphology, suggesting that XBPs can indeed be attributed to magnetic reconnection. The models used, however, are purely geometric and make no predictions about energies. Furthermore, each study analyzed specific XBPs, and did not make any general predictions concerning interaction distances in three dimensions.

Recently a model called the *minimum current corona* (MCC, Longcope 1996) has quantified the basic geometric three dimensional reconnection models. It predicts the induction of current along separator field lines. This current stores energy which is liberated if and when fast magnetic reconnection occurs.

The present work applies MCC to the case of a magnetic bipole. This leads to predictions for the interaction distance and heating power for magnetic bipoles in every possible configuration. The predicted size and power compare favorably to the values inferred from observations of XBPs. The exact scaling can be tested against existing or future XBP data. Furthermore, the model leads to several other predictions, such as an angular discrepancy between the axis of the bipole and the XBP, which can be tested.

2. A model bipole

A magnetic bipole consists of a positive and a negative pole, of fluxes ψ_+ and ψ_-, separated by a distance d. The poles may be linked to one another by coronal magnetic field lines, and they may also be linked to other sources of flux such as more distant small poles, or larger sources such as active regions. We will treat all other sources of flux as an overlying or *background field*, whose origin is assumed far away compared to d. The scale of variation in the background field will be large compared to d and it can be approximated as uniform and horizontal, with magnitude B_0.

Our model of a magnetic bipole consists of two point sources of flux (magnetic charges) denoted P and N, resting on the horizontal plane $z = 0$ (fig. 1). The poles are located at positions $\mathbf{x}_+$ and $\mathbf{x}_-$, separated by a distance d. The axis of the bipole (directed from P to N) makes an angle ϕ with respect to the background field vector $\mathbf{B}_0$. For a current-free (vacuum) corona the magnetic field can be written by analogy to electrostatics

$$\mathbf{B}(\mathbf{x}) = \frac{\psi_+}{2\pi}\frac{\mathbf{x}-\mathbf{x}_+}{|\mathbf{x}-\mathbf{x}_+|^3} - \frac{\psi_-}{2\pi}\frac{\mathbf{x}-\mathbf{x}_-}{|\mathbf{x}-\mathbf{x}_-|^3} + \mathbf{B}_0 \quad . \tag{1}$$

The magnetic charge of each source is $q_\pm = \pm\psi_\pm/2\pi$ so that the designated flux enters the corona from each one.

We define a coordinate system whose origin is midway between charges, and with $\hat{\mathbf{x}}$ directed along the background field vector $\mathbf{B}_0$. For simplicity we will restrict consideration to bipoles of matched flux

$$\psi_+ = \psi_- = \psi_0 \quad .$$

This defines the characteristic flux which we use to scale our equations. With the background field strength, B_0, we define a characteristic length scale

$$\ell \;\equiv\; \sqrt{\psi_0/B_0} \;=\; 10\;\psi_{19}^{1/2}\,B_1^{-1/2}\;\mathrm{Mm} \quad , \tag{2}$$

where ψ_{19} and B_1 are the values of ψ_0 and B_0 in units of 10^{19} Mx, and 10 Gauss respectively.

Using ψ_0, B_0 and ℓ to scale eq. (1) gives the dimensionless magnetic field

$$\mathbf{B}(\mathbf{x}) = \frac{1}{2\pi}\frac{\mathbf{x}-\mathbf{x}_+}{|\mathbf{x}-\mathbf{x}_+|^3} \;-\; \frac{1}{2\pi}\frac{\mathbf{x}-\mathbf{x}_-}{|\mathbf{x}-\mathbf{x}_-|^3} \;+\; \hat{\mathbf{x}} \quad , \tag{3}$$

where by choice of coordinates $\mathbf{x}_- = -\mathbf{x}_+$. The bipole is entirely characterized by the dimensionless separation vector

$$\boldsymbol{\rho} \;\equiv\; \tfrac{1}{2}\,\ell^{-1}\,(\mathbf{x}_- - \mathbf{x}_+) \;=\; \ell^{-1}\,\mathbf{x}_- \tag{4}$$

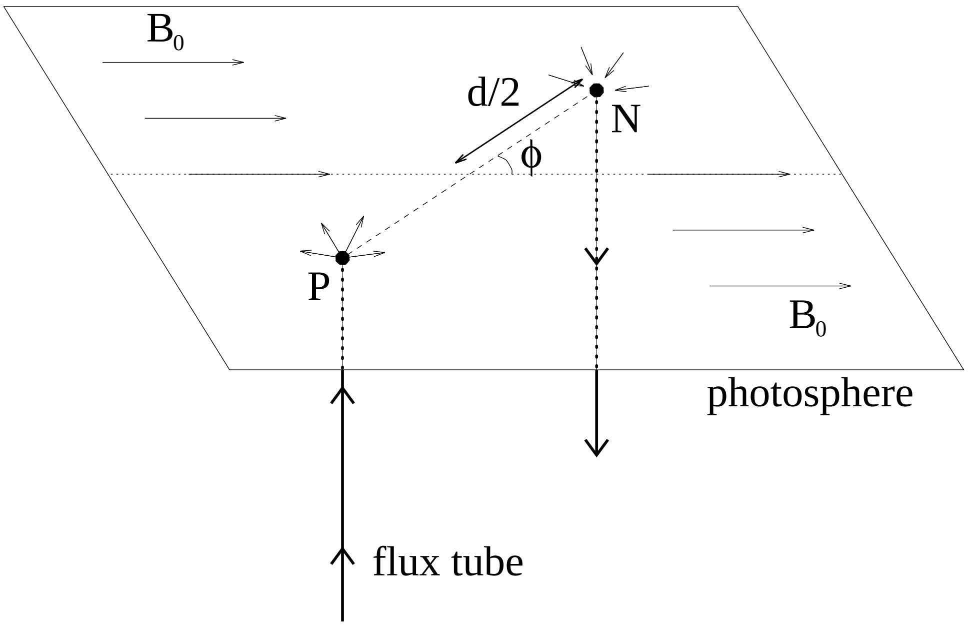

Fig. 1.— The geometry of the model bipole. The uniform background field is taken as the $\hat{\mathbf{x}}$ direction. The bipole consists of point charges separated by d making an angle ϕ with the background field.

directed from P to N. This two dimensional vector is the entire parameter space for the configurations of the bipole. Its magnitude describes the dimensionless separation

$$\rho \ = \ \tfrac{1}{2}d/\ell \ = \ \tfrac{1}{2}\sqrt{B_0 d^2/\psi_0} \ ,$$

and its polar angle ϕ is the angle of the bipole relative to the background field. The remainder of this work explores the full two dimensional parameter space of magnetic bipoles.

Magnetic field lines from eq. (3) may be traced numerically both forwards and backwards from any point, to their ultimate beginnings or ends. With a few notable exceptions each magnetic field line must fall into one of four categories according to where it begins and ends (see fig. 2). Those field lines which begin at P and end at N form the bipole itself. There are also field lines which begin at P and then extend to ∞, thereby linking P to the background field. Similarly there are field lines beginning at ∞ and ending at N. And finally, there are purely background field lines which begin and end at ∞, never encountering a pole (not shown in fig. 2). These different categories of field lines define four spatial domains which we call P–N, P–∞, ∞–N and ∞–∞ respectively. These domains are separated from one another by surfaces called separatrices.

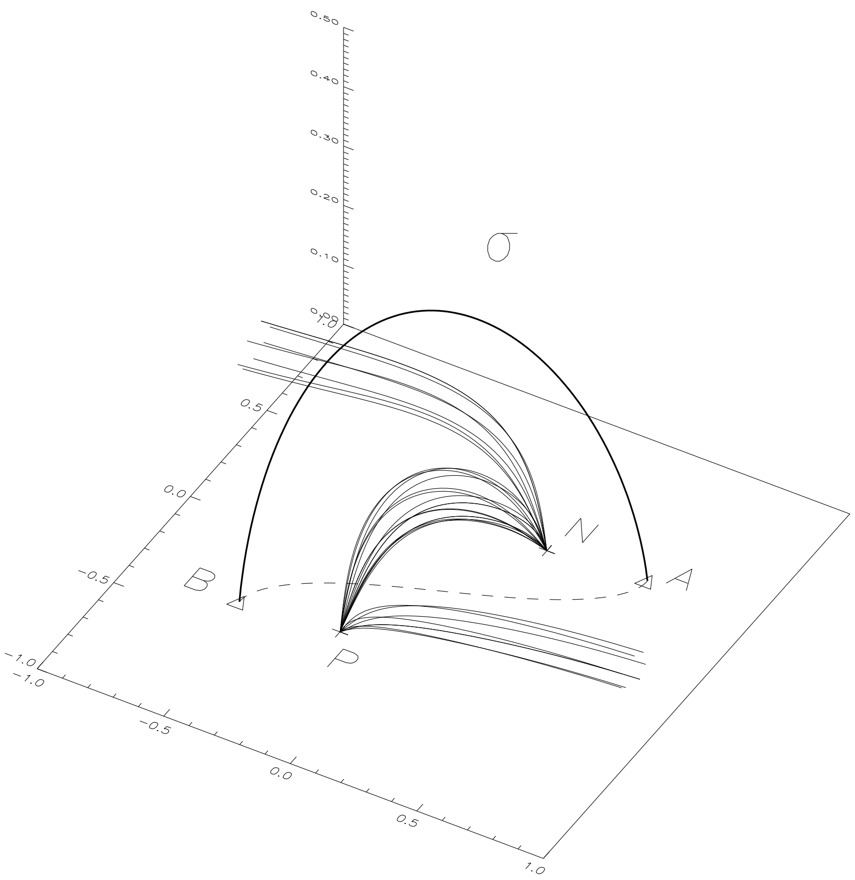

Fig. 2.— Some example field lines for the model bipole. Shown are clusters of field lines from domains P–N, ∞–N and P–∞. Also show is the separator σ (solid) and the return path in the photosphere (dashed).

The domains P–N and ∞–N differ from the domains P–∞ and ∞–∞ by the end-points of their field lines. Separating these two pairs of domains is a surface consisting of field lines which neither end at the charge N nor continue indefinitely. Instead the field lines on this surface end at a magnetic null point (i.e. where $\mathbf{B}(\mathbf{x}) = 0$) called A. This is the separatrix surface Σ_A and it forms an approximate paraboloid (fig. 3a) inside of which all field lines terminate at N, outside of which all field lines continue to ∞. Note that P lies on this surface since Σ_A consists partly of field lines beginning at P. There is a second separatrix Σ_B whose field lines begin at a second magnetic null (B). Inside Σ_B all field lines begin at P and this surface divides P–N and P–∞ from ∞–N and ∞–∞.

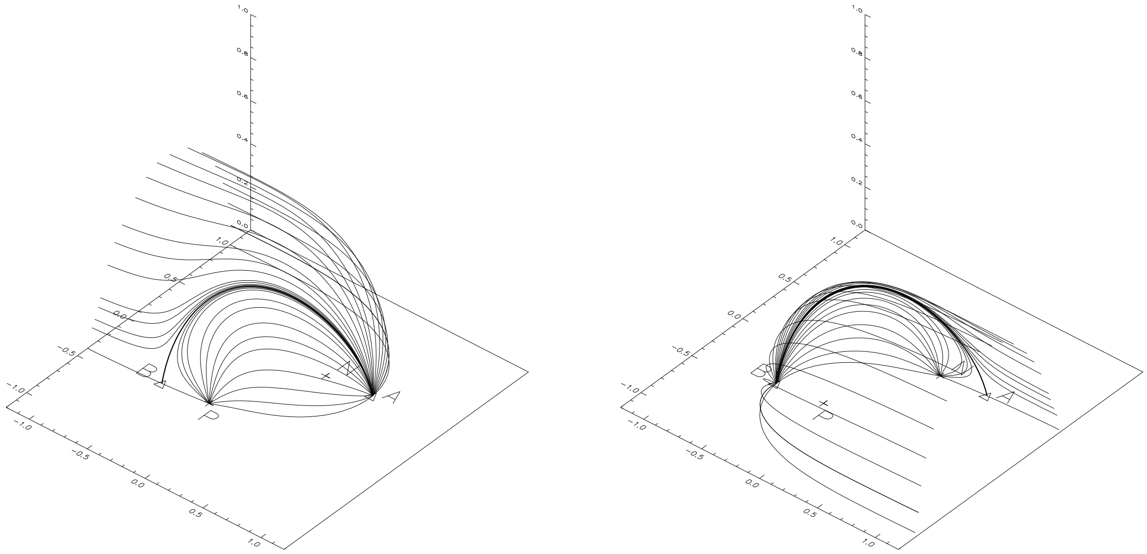

Fig. 3.— Field lines from the two separatrix surfaces. (a) Σ_A (b) Σ_B.

Together the two surfaces Σ_A and Σ_B divide the coronal volume into its four domains. The domain P–N lies simultaneously within both paraboloids; it constitutes the bipole. There is a single field line, called the *separator* σ, which forms the intersection of the surfaces. Perforce this field line must begin at the null B and end at the null A. We can incorporate σ into a closed loop $\mathcal{C}$ using a return path within the photosphere (see fig. 2). This closed loop encircles the flux in domain P–N and no other flux.

Taking advantage of $\mathcal{C}$ we can calculate the net flux inside domain P–N, to be denoted $\hat{\psi}$,

$$\hat{\psi} \;=\; \oint_{\mathcal{C}} \mathbf{A}\cdot d\mathbf{l} \quad , \tag{5}$$

where $\mathbf{A}$ is the magnetic vector potential. The direction of integration is taken to be from B to A in the corona, which makes $\hat{\psi}$ non-negative. Since the flux in each tube is unity in our rescaled variables $0 \leq \hat{\psi} \leq 1$. The total flux linking P to N is $\Psi_{PN} = \psi_0 \, \hat{\psi}$ in original units.

In each configuration of the poles, parameterized by $\boldsymbol{\rho}$, the amount of shared flux $\hat{\psi}$ will be different. In some configurations, for instance if N is far to the left of P, the paraboloids Σ_A and Σ_B do not intersect at all and $\hat{\psi} = 0$. In these cases there are no field lines connecting P to N, hence there is no bipole. Conversely, in the configurations for which $\hat{\psi} > 0$ the poles do share flux, and can interact with one another; this will be called *the interaction region* in parameter space. The boundary of the interaction region will be denoted $\rho_{\rm int}(\phi)$.

Using the current-free field, given by eq. (3) for each configuration, it is possible to defined the shared flux as a function we denote $\hat{\psi}^{(\rm v)}(\boldsymbol{\rho})$ to emphasize the use of a vacuum field. For a specific value of $\boldsymbol{\rho}$ the magnetic field in eq. (3) is used, with $\mathbf{x}_+ = -\boldsymbol{\rho}$ and $\mathbf{x}_- = \boldsymbol{\rho}$. The separator field line is located numerically using an algorithm described in Longcope 1996. Equation (5) is then used to calculate $\hat{\psi}^{(\rm v)}$ for this value of $\boldsymbol{\rho}$. This procedure is repeated for a grid of configurations $\boldsymbol{\rho}$. Figure 4 shows contours of $\hat{\psi}^{(\rm v)}$ resulting from this procedure. A dark contour marks $\rho_{\rm int}$, the boundary of the interaction region, outside of which $\hat{\psi}^{(\rm v)} = 0$ everywhere. The $\hat{\psi}^{(\rm v)} = 1$ contour follows the the $\phi = 0$ line beginning at the origin. Along this line symmetry dictates that the sources be completely interlinked. At every other point inside the interaction region the sources are only partially interlinked and all four flux domains exist.

Outside the interaction region there is no bipole, and therefor no XBP. Thus we find that only those poles separated by distances

$$d < 2\ell \, \rho_{\rm int}(\phi) \;\simeq\; \sqrt{\psi_0/B_0} \;=\; 10\, \psi_{19}^{1/2} \, B_1^{-1/2} \, {\rm Mm} \quad , \tag{6}$$

can form XBPs. The interaction boundary $\rho_{\rm int}(\phi)$ depends on the angle of the bipole, but is typically $\rho_{\rm int} \sim 0.5$. The maximum separation d depends on the flux in the poles and also on the strength of the background (overlying) field; in the absence of a background field ($B_0 = 0$) the poles would have no alternative but to interact with each other, thus the interaction distance is ∞.

3. Evolution of the bipole

As the two poles, P and N, move across the photosphere the parameters of the bipole will change: $\boldsymbol{\rho}(t)$. This motion will be convergent (i.e. cancellation) if $\dot{\rho} < 0$

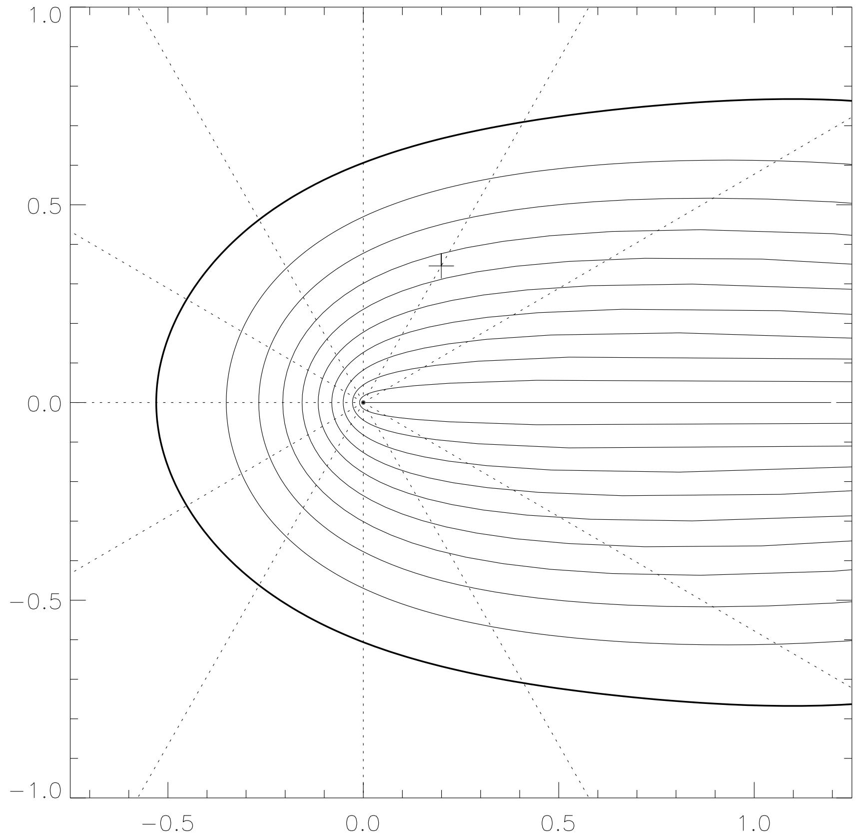

Fig. 4.— Contours of the function $\hat{\psi}^{(\mathrm{v})}(\boldsymbol{\rho})$. The contour interval is 0.1 with the outer contour representing the boundary of the interaction region $\rho_{\mathrm{int}}(\phi)$. The + marks the configuration of the bipole shown in fig. 2; for this case $\hat{\psi}^{(\mathrm{v})} = 0.348$. The horizontal line along the right of the ρ_x axis is the $\hat{\psi}^{(\mathrm{v})} = 1$ contour where the two poles are entirely linked.

and divergent (i.e. emergence) if $\dot{\rho} > 0$. For the corona to remain current-free in the face of the polar motion would require the flux $\hat{\psi}$ to change in time

$$\frac{d\hat{\psi}}{dt} \;=\; \dot{\boldsymbol{\rho}} \cdot \nabla \hat{\psi}^{(\mathrm{v})} \quad , \tag{7}$$

where ∇ denotes derivatives with respect to the components of $\boldsymbol{\rho}$.

A changing flux, however, requires an electric field according to Faraday's law. In this case the electric field would have to occur along the separator σ

$$\frac{d\hat{\psi}}{dt} = -c \int_B^A E_{\parallel}\, dl \quad , \tag{8}$$

since the photosphere is effectively a conductor, supporting no tangential field. (The conductive nature of the photosphere reflects its empirical tendency to exclude coronal flux, rather than its intrinsic resistivity [see Longcope 1996]). A velocity of 300 m/s would require electric field $E_{\parallel} \simeq 0.3\,\mathrm{V/m}$ to accomplish the necessary reconnection. This is above the Dreicer field for the coronal plasma, 0.03 V/m, and is not easily supported without a large coronal current density and anomalous resistivity.

Longcope and Cowley (1996) proposed that such a system evolves into force-free equilibria with current flowing in a singular ribbon roughly paralleling the separator. There is also a return current along the photosphere. The current I gives rise to a self-flux $\hat{\psi}^{(\mathrm{cr})}(I)$ which keeps the total flux in domain P–N constant

$$\hat{\psi} \;=\; \hat{\psi}^{(\mathrm{v})}(\boldsymbol{\rho}) \;+\; \hat{\psi}^{(\mathrm{cr})}(I) \;=\; \mathrm{const} \quad . \tag{9}$$

Longcope (1996) estimated the current-flux relationship, in the limit of small $|I|$, to be

$$\hat{\psi}^{(\mathrm{cr})}(I) \;=\; \frac{LI}{c} \ln[\,256 e^{-3} I^{\star}/|I|\,] \;=\; \frac{LI^{\star}}{c} \Lambda(I/I^{\star}) \quad , \tag{10}$$

where L is the length of the separator, and $\Lambda(x) = x \ln(256e^{-3}/|x|)$. The fiducial current $I^{\star}(\boldsymbol{\rho})$ relates to the shear in the vacuum magnetic field averaged along the separator, according to a prescription in Longcope (1996). Most notably, these quantities depend only on the current-free field and can be numerically determined as functions of $\boldsymbol{\rho}$ at the same time as $\hat{\psi}^{(\mathrm{v})}(\boldsymbol{\rho})$.

Inverting equation (9) gives the current I which is induced by changes in the bipole parameters $\boldsymbol{\rho}$. This current flows in a singular ribbon to produce a force-free magnetic field with the prescribed amount of linking flux $\hat{\psi}$. This field necessarily has a larger magnetic energy than the current-free field for the same values of ρ and ϕ. The difference in energy is (Longcope 1996)

$$\Delta\mathcal{E} \;=\; \frac{1}{c}\int_0^{\hat{\psi}^{(\mathrm{cr})}(I)} I(\psi)\,d\psi \;=\; \frac{L}{2c^2}I^2\ln[\,256e^{-7/2}\,\frac{I^\star}{|I|}\,] \ , \tag{11}$$

as it would be for any inductor. This free energy is attributable to the presence of the current. The energy density is not, however, localized to the current ribbon, rather it takes the form of a roughly dipolar magnetic field extending over the whole corona.

4. Reconnection and energetics

4.1. The stick-slip reconnection model

Reconnection is a process whereby an electric field $E_{\parallel}$ is generated along the current ribbon permitting $\hat{\psi}$ to change. While significant electric fields do not occur under quiescent conditions, there are a variety of instabilities to which a current ribbon might be susceptible. Any one of these instabilities would generate anomalous resistivity thus causing reconnection (Syrovatskii 1981, Somov 1992). Rather than dwell on details we will assume that some instability will occur if the current exceeds a threshold $\theta I^\star$ (Longcope 1996). The dimensionless parameter θ depends on the nature of the instability; in what follows we set it to various values less than unity. Once triggered, the effect of the reconnection is to transfer enough flux across the separator that $\hat{\psi} \to \hat{\psi}^{(\mathrm{v})}(\boldsymbol{\rho})$ and the current ribbon disappears.

As a result of reconnection the coronal field assumes a new equilibrium whose energy is lower by exactly the amount in eq. (11). The fate of this energy cannot be determined from our quasi-static model. If the magnetic field is ever to assume an equilibrium again, however, the energy must be dissipated. This dissipation presumably heats the coronal plasma and evaporates chromospheric plasma, giving rise to a sudden X-ray brightening in the vicinity of the separator. We therefore associate the reconnection event with an XBP.

As the poles continue to move current will again build up until it reaches the threshold and causes another instance of reconnection and accompanying loop brightening. This is the model of *stick-slip* reconnection introduced by Longcope 1996. The corona acts intermittently as a conductor, which prohibits reconnection, and then as a resistor, which permits it. During this process there are sporadic releases of energy into the coronal plasma.

To demonstrate this scenario consider a bipole undergoing cancellation (i.e. cconvergence of the poles) along an axis making an angle of $\phi = 120°$ with respect to the background. Take the values $B_0 = 10$ G and $\psi_0 = 10^{19}$ Mx for which $\ell = 10^9$ cm. Each pole is moving at $v = 300\,\mathrm{m/s}$, so that the dimensionless speed is $\dot{\rho} = 3 \times 10^{-5}\,\mathrm{sec}^{-1}$. The interaction distance $\rho_{\rm int}(120°) \simeq 0.5$ means that the bipole should completely cancel in $t = \rho_{\rm int}/\dot{\rho} \simeq 1.7 \times 10^4$ sec (5 hours) after their coronal fields first encounter one another. Finally, we set the threshold coefficient to $\theta = 0.15$, as in Longcope 1996.

In the resulting time history the bipolar flux Ψ_{PN} manages to follow the vacuum value $\psi_0\,\hat{\psi}^{(\rm v)}$ in a stair-step fashion (fig. 5c). Each step transfers $\sim 10^{18}$ Mx $= 10^{10}$ Volt–sec by a single a reconnection event. The events, occurring once every $\sim$ 30 minutes, release the accumulated free energy (fig. 5d). The time history begins when the bipole enters the interaction distance and ends $\sim$ 5 hours later.

4.2. Reconnection frequency

By the end of the above cancellation the two flux tubes have gone from being magnetically isolated ($\hat{\psi} = 0$) to magnetically coupled ($\hat{\psi} = 1$). Once they are entirely coupled they may be removed, possibly by subduction, without affecting the overlying field. This transition occurs through a series reconnection events each of which involves thermalization of temporarily stored magnetic energy. The average interval Δt between events is the time necessary for the change in $\hat{\psi}^{(\rm v)}$ to reach the threshold for current ribbon self-flux

$$\Delta\hat{\psi}^{(\rm v)} ~=~ |\dot{\boldsymbol{\rho}}\cdot\nabla\hat{\psi}^{(\rm v)}|\,\Delta t ~\simeq~ \hat{\psi}^{(\rm cr)}(\theta\, I^{\star}) ~=~ \frac{I^{\star}L}{c}\,\Lambda(\theta) \quad . \tag{12}$$

Denoting by ζ the angle between $\dot{\boldsymbol{\rho}}$ and the gradient $\nabla\hat{\psi}^{(\rm v)}$ we can write the distance $\Delta\rho$ moved by the poles before a reconnection event

$$\Delta\rho = \frac{I^{\star}L/c}{|\nabla\hat{\psi}^{(\rm v)}|}\,\frac{\Lambda(\theta)}{\cos\zeta} = \frac{\Lambda(\theta)}{\cos\zeta}\,\Delta\rho_0 \quad . \tag{13}$$

The quantity $\Delta\rho_0$ depends only on the bipole configuration $\boldsymbol{\rho}$. Numerical evaluation shows that it is typically $\Delta\rho_0 \sim 0.075$ away from the origin; this is in units of ℓ. In the example above, using $\Lambda(0.15) = 0.67$, we find $\Delta t \simeq \Delta\rho/\dot{\rho} \simeq 1.5 \times 10^3$ sec (30 minutes), consistent with fig. 5e.

Histories of the same cancellation event, but using different values of the threshold parameter θ, are shown in figs. 6. The larger the threshold value, the

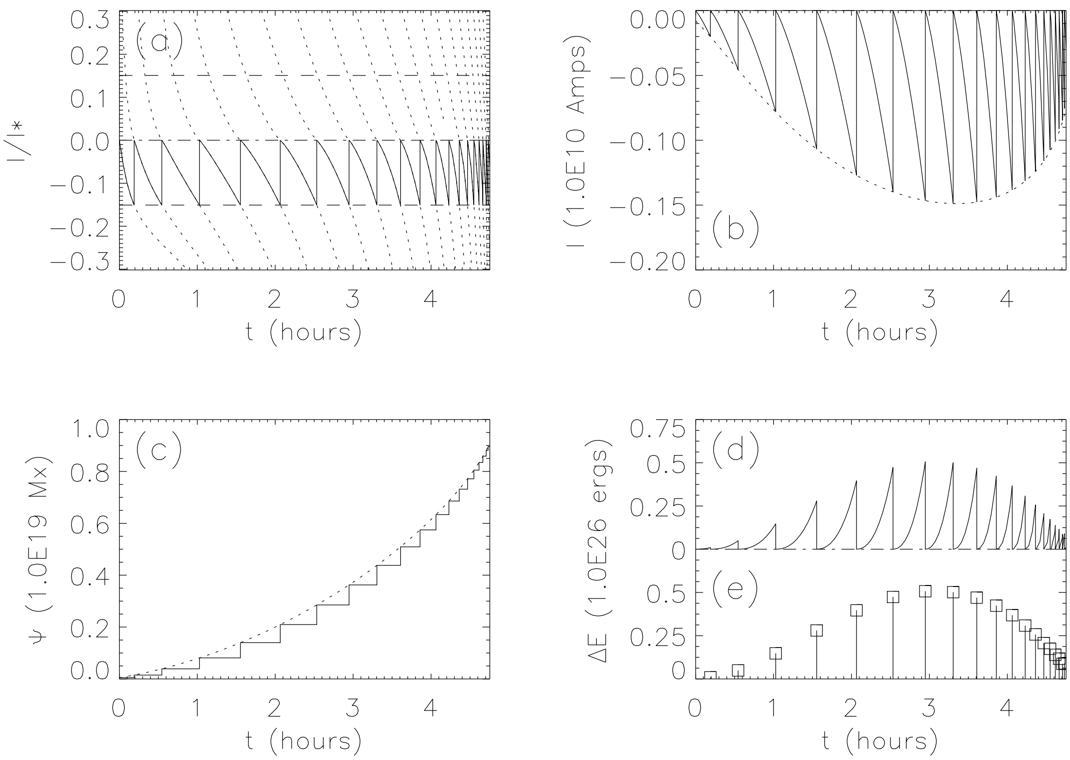

Fig. 5.— The time history of a bipole during convergence along the trajectory $\phi = 120°$. (a) The ratio $I/I^{\star}$. When the magnitude of this quantity exceeds $\theta = 0.15$ reconnection occurs. (b) The current I in units of 10^{10} A. (c) The linked flux Ψ_{PN} in units of 10^{19} Mx (ψ_0). (d) The free energy $\Delta\mathcal{E}$ and (e) a depiction of the energy liberated during each reconnection event.

larger the interval between reconnection events, and the larger the energy released by each event. Once again Δt agrees with the general expression in eq. (12).

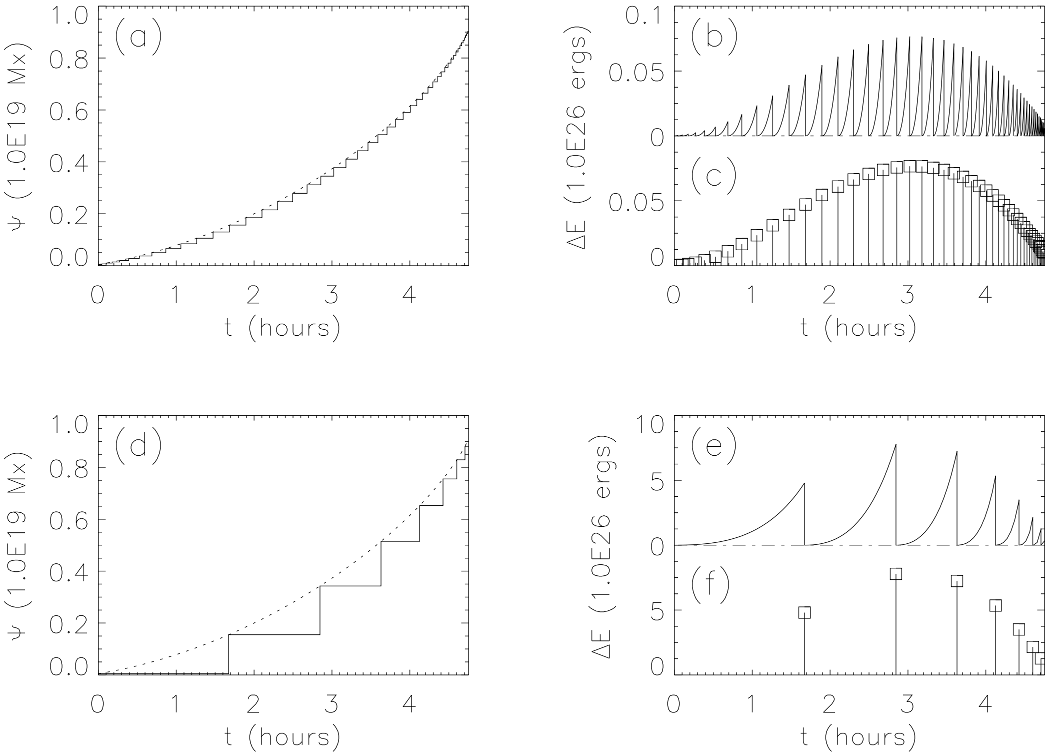

Fig. 6.— Time histories of the same cancellation event with different thresholds. (a)–(c) $\theta = 0.05$, (d)–(f) $\theta = 0.5$. Note that the scales for flux are the same, while the scales for the energies differ by two orders of magnitude (and differ from that in figs. 5d and 5e).

According to the stick-slip model, reconnection releases magnetic energy in repeated impulses. The evolution of a plasma subject to impulsive heating, sometimes called "nanoflaring", has been the subject of several investigations (Cargill 1994). The principle issue is the time $\tau_{\rm cool}$ taken for the plasma to cool either by radiation or thermal conduction to the chromosphere. If the heating occurs at intervals $\Delta t < \tau_{\rm cool}$ then the plasma will radiate continuously; the impulsive nature of the heating will be obscured. If, on the other hand, $\Delta t > \tau_{\rm cool}$ then the plasma will cool between impulses, and its luminosity will fluctuate over time. In this case the loop will appear bright for only a fraction of the time

$$f = \frac{\tau_{\rm cool}}{\Delta t} \; = \; \frac{\tau_{\rm cool}\,\dot{\rho}}{\Delta\rho_0}\,\frac{\cos\zeta}{\Lambda(\theta)} \; \simeq \; 13 \times \tau_{\rm cool}\, v\, \psi_0^{-1/2}\, B_0^{1/2}\, \Lambda(\theta) \quad , \tag{14}$$

where we have taken $\Delta\rho_0 = 0.075$. The case $\Delta t < \tau_{\rm cool}$ leads to $f > 1$ indicating that the loop is visible all the time.

4.3. Energetics

The energetic cost of forging links between the converging poles can be found by adding up the released energies; in fig. 5e this gives 5×10^{26} ergs. Alternatively, we can divide the energy $\Delta\mathcal{E}$ released at threshold by the interval Δt between events (i.e. [12]) to get a general expression for average heating power (Longcope 1996)

$$\bar{\mathcal{P}} \simeq \frac{\theta}{2c} I^\star \left| \frac{d\hat{\psi}^{(\rm v)}}{dt} \right| ~=~ \theta \left| \frac{I^\star}{2c} \dot{\boldsymbol{\rho}} \cdot \nabla \hat{\psi}^{(\rm v)} \right| ~\equiv~ \theta |\, \dot{\boldsymbol{\rho}} \cdot \mathbf{F} \,| ~~. \qquad (15)$$

We have introduced the force vector $\mathbf{F}(\boldsymbol{\rho})$ depending only on the bipole configuration. Since the heating power is linear in velocity $\dot{\boldsymbol{\rho}}$, and always positive, the force is analogous to a mechanical friction (Marion & Thornton 1988). The actual power released is linearly proportional to the reconnection efficiency θ.

Like a mechanical friction force $\mathbf{F}$ does not depend on the magnitude of the velocity $\dot{\boldsymbol{\rho}}$, but does depend on its direction: the force always counteracts the motion. The flux tubes feel this force due to the accumulation of coronal current. They also feel an attractive force

$$|\mathbf{F}_{\rm pot}| = \tfrac{1}{2} \frac{q_+ q_-}{d^2} = \frac{\psi_0^2}{8\pi^2 d^2} = \psi_0 \, B_0 \, \frac{1}{32\pi^2 \rho^2}$$

due purely to the potential field. Once again this has a direct analogy in electrostatics, however, the factor $\frac{1}{2}$ arises because the force can only act in the half-space above $z = 0$. Below the solar surface the flux tubes are confined and do not influence each other magnetically. The force arises because the energy in the potential field decreases as the charges approach. This is a reversible process so it will not lead to heating of the corona.

By far the most important force acting on a flux tube is imparted to it from motions in the convection zone. These forces push the flux tube, causing its top at $\mathbf{x}_\pm$ to move in a seemingly prescribed fashion. Thus we will treat the motion $\dot{\boldsymbol{\rho}}$ as a prescribed quantity, not subject to the coronal forces $\mathbf{F}$ or $\mathbf{F}_{\rm pot}$. The importance of the force $\mathbf{F}$ is that it dictates the heating delivered to the corona by the flux tube motion.

Figure 7 shows contours of the magnitude $|\mathbf{F}(\boldsymbol{\rho})|$. The direction of the vector is normal to the contours of $\hat{\psi}^{(\rm v)}$ (fig. 4); if $\boldsymbol{\rho}(t)$ follows a contour then $\bar{\mathcal{P}} = 0$ since no reconnection occurs. Typical values near the middle of the interaction region are $|\mathbf{F}| \sim 0.1$ in our dimensionless units. (The potential force is $|\mathbf{F}_{\rm pot}| \simeq 0.1$ at a similar radius, $\rho \simeq 0.2$. This means that friction forces are smaller than potential forces by $\sim \theta$.). The typical heating power dissipated by $\mathbf{F}$ is

$$\bar{\mathcal{P}} \;\simeq\; 0.1\,\theta\,\psi_0\,B_0\,v \;=\; \theta\,\psi_{19}\,B_1\,v_4 \;\times\; 10^{23}\,{\rm erg/sec} \tag{16}$$

where v_4 is the velocity in units of 100 m/sec. In the example from fig. 5 ($\theta = 0.15$ and $v_4 = 3$) this gives $\bar{\mathcal{P}} \simeq 5 \times 10^{22}$ erg/sec. This heating takes the form of impulses $\Delta\mathcal{E} \sim 5 \times 10^{25}$ erg occurring every $\Delta t \sim 10^3$ seconds. Toward the end of the example the impulses grow smaller, but more frequent. The net effect is a slightly larger $\bar{\mathcal{P}}$, as indicated by the maximum in $|\mathbf{F}|$ near the origin.

The model above provides a quantitative theory for the energy dissipated by the cancellation of two magnetic poles. The exact same energy would be dissipated by *emergence* along the same path. The friction-like force, however, is non-conservative so the liberated energy does depend on the path. Figure 8 shows quantities for poles moving along radial paths at different angles ϕ. The interval between events, $\Delta\rho_0/\cos\zeta$, is shown in fig. 8a, while the radial component of the friction, $\hat{\boldsymbol{\rho}}\cdot\mathbf{F}$, is shown in 8b. Note that in most cases the maximum force is at the origin $\rho = 0$. If liberated power is correlated with X-ray luminosity, then we should expect XBPs to be brightest (in absolute terms) when they are smallest.

The total energy from reconnection is found from the time integral of $\bar{\mathcal{P}}$. For the radial paths above this energy becomes

$$\mathcal{E} = \int \bar{\mathcal{P}}\,dt = \theta \int F(\rho)\,\dot{\rho}\,dt = \theta \int_0^{\rho_{\rm int}} F(\rho)\,d\rho \quad . \tag{17}$$

Figure 9 shows $\mathcal{E}/\theta$ versus the angle of the path ϕ. Its magnitude, $\mathcal{E}/\theta \sim 0.035$, is remarkably constant over different angles. This means that the complete cancellation (or emergence) of two magnetic poles releases an energy

$$\mathcal{E} \simeq 0.035\,\theta\,\psi_0^{3/2}\,B_0^{1/2} \;=\; \theta\,\psi_{19}^{3/2}\,B_1^{1/2}\;3.5 \times 10^{27}\,{\rm ergs} \quad . \tag{18}$$

For the example in fig. 5 ($\theta = 0.15$) this general formula gives $\mathcal{E} = 5 \times 10^{26}$ ergs, exactly the same as adding up all the energy releases.

5. Morphology of X-ray bright points

The model above attributes XBPs to reconnection in a magnetic bipole. We have shown that reconnection would naturally liberate magnetic energy, which would

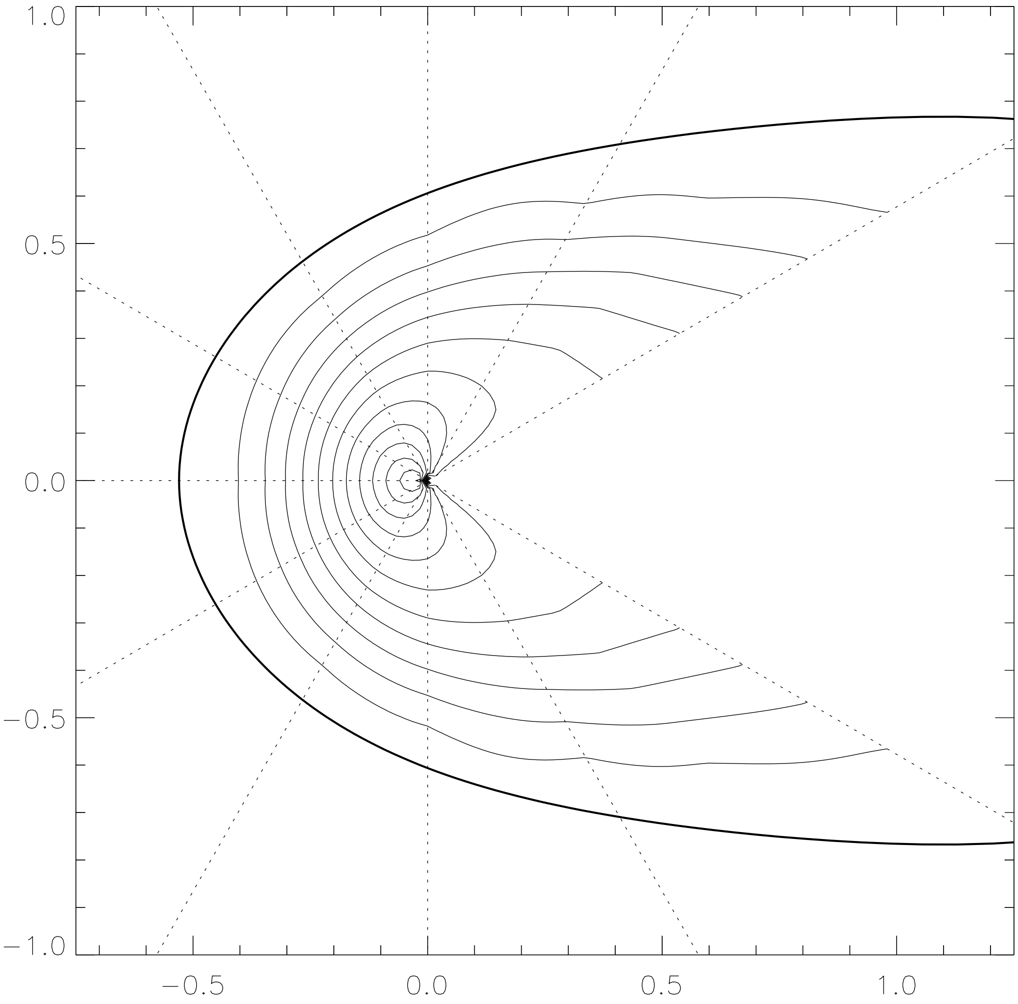

Fig. 7.— Contours of the magnitude of the reconnection force $|\mathbf{F}(\boldsymbol{\rho})|$. Contour intervals are 0.015. Inside the wedge $|\phi| < 30^\circ$ the current $I^\star$ is difficult to calculate.

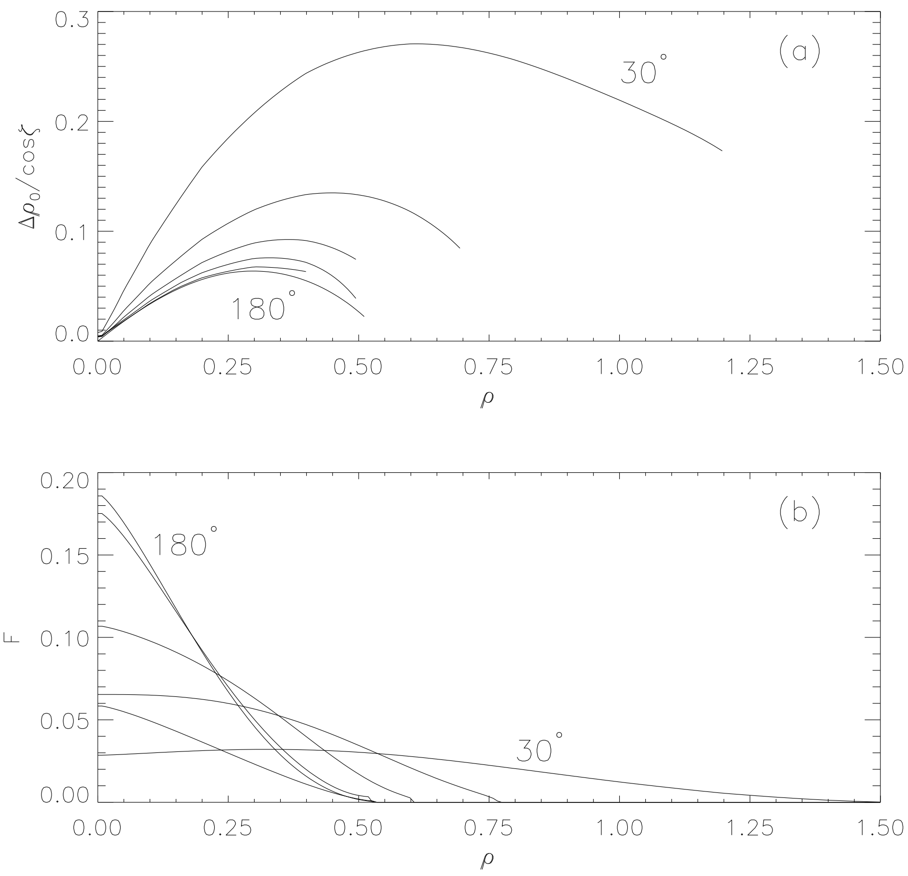

Fig. 8.— Values of (a) $\Delta\rho_0/\cos\zeta$ and (b) the radial component of **F** for radial paths at angles $\phi = 30°$, $60°$, $90°$, $120°$, $150°$, $180°$.

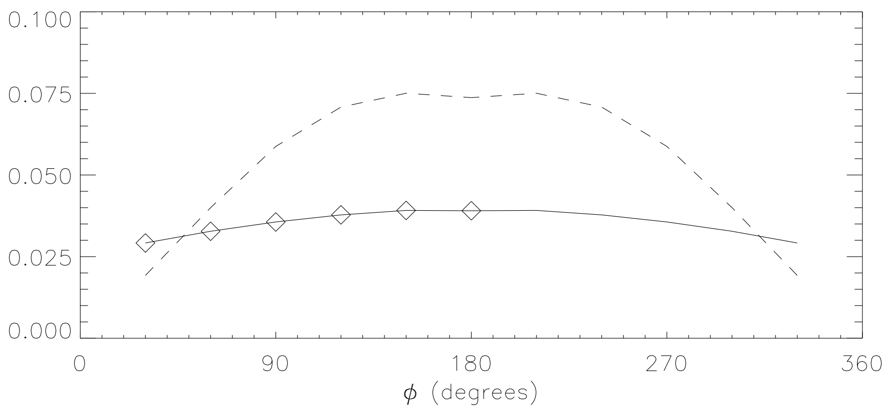

Fig. 9.— Total energy $\mathcal{E}/\theta$ released (solid) by cancellation (or emergence) along the radial path defined by angle ϕ. The diamonds mark the curves from fig. 8b which were integrated. The dashed line gives the average force experienced over this path.

in turn, lead to X-ray brightening along affected magnetic field lines. The magnetic field lines most affected will be those closest to the reconnection site: the separator field line σ. Thus we expect the morphology of an XBP to reflect the morphology of the separator.

Viewed from above (see fig. 10) the separator makes a lazy "S" shape connecting the two null points (fig. 10). It is worth recalling that a potential magnetic field being used so the curvature cannot be the result of current (Priest & Milne 1980). The magnetic field is sheared, even in this potential field. At low altitudes the magnetic field is directed along the bipole axis, while higher up the background field dominates. The separator σ follows each of these directions over its length, leading to its S shape. *The axis of the separator is intermediate between the bipole and the background.*

This S-shaped separator makes an angle $\Delta\phi$ with respect to the axis of the bipole itself (i.e. P and N) since its ends, the null points, are necessarily offset from the poles. This offset angle is an important prediction of the separator model; simpler models do not often distinguish between the bipole and the X-ray loop. Significantly such an offset has been noted in observations of X-ray bright points (Kankelborg et al. 1996). Important constraints may be placed on the separator model by measurements of these offset angles.

The value of the theoretical offset angle depends on the definiton of the separator axis. Defining a separator axis connecting the null points leads to an offset

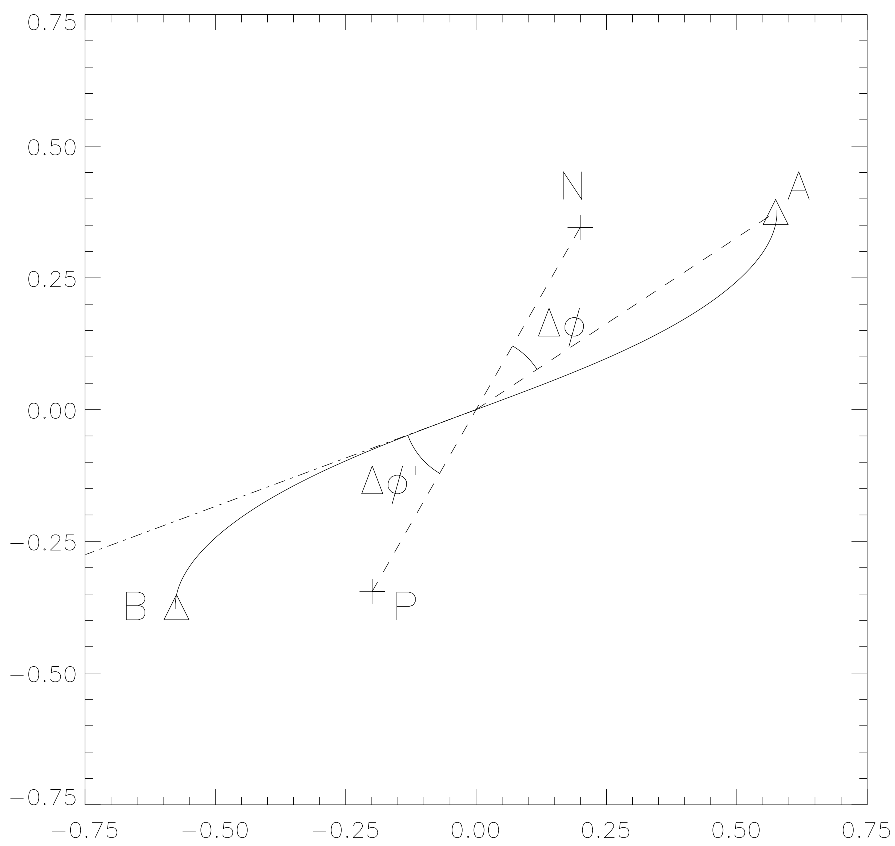

Fig. 10.— The separator field line, viewed from above, for a bipole $\rho = 1$, $\theta = 60°$. The axis of the bipole is shown as a dashed line. Also shown are two definitions of the separator axis (dashed and broken) leading to the two offset angles $\Delta\phi$ and $\Delta\phi'$.

$\Delta\phi$. Choosing the apex of the separator leads to a different angle $\Delta\phi'$ (see fig. 10). In practice these two offsets are not very different. Figure 11 shows the direction of each axis at different points in parameter space. The offset $\Delta\phi$ corresponds to the angle between this axis and the radial. For angles $|\phi| > 90°$ these offsets can be significant, becoming $\Delta\phi = \Delta\phi' = 90°$ at the $\phi = 180°$ line. Conversely, when the the bipole and the background are nearly alinged, $|\phi| < 90°$ the offset angle is not great.

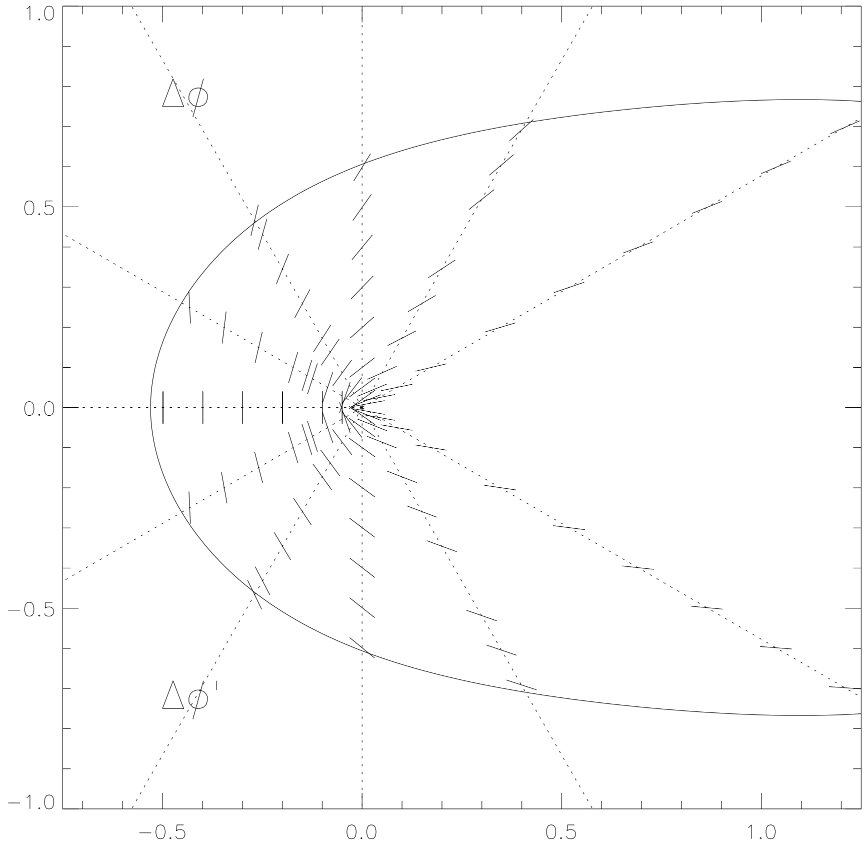

Fig. 11.— Axis of the separator throughout configuration space $\boldsymbol{\rho}$. The two definitions of this axis are shown in the $\phi > 0$ and $\phi < 0$ portion of the graph.

6. Conclusion

6.1. Summary

We have presented a model for the interaction of two opposite magnetic poles, each of flux ψ_0. This interaction, due to the relative motion of the poles, at velocity v, can take the form of a collision and cancellation, an emergence and separation, or a grazing encounter. The poles exist in a background magnetic field of strength B_0. Their interaction consists of disconnecting coronal field lines from from the background field, and reconnecting them to each other (in the case of cancellation), or *vice versa*. Without the background field there would be no "interaction"; the poles would be always connected to one another. The reconnection is assumed to proceed due to a plasma instability triggered when coronal current exceeds a threshold, paramterized by the dimensionless quantity θ.

The interaction described above can be fully characterized in terms of a dimensionless configuration parameter $\boldsymbol{\rho}$, and its rate of change $\dot{\boldsymbol{\rho}}$. For typical configurations we find that poles will begin to interact once their separation is less than the interaction distance

$$d \;\leq\; \psi_0^{1/2}\,B_0^{-1/2} \quad . \tag{19}$$

The poles will interact for a time

$$t_{\rm life} \;\simeq\; \tfrac{1}{2}d/v \;=\; \tfrac{1}{2}\psi_0^{1/2}\,B_0^{-1/2}\,v^{-1} \quad , \tag{20}$$

which can be taken as the lifetime of an XBP. The stick-slip reconnection process stores, and then dissipates magnetic energy. This results in a mean dissipated power (at peak luminosity) of

$$\bar{\mathcal{P}} \;\simeq\; 0.1\,\theta\,\psi_0\,B_0\,v \quad . \tag{21}$$

During its lifetime the XBP will dissipate a total energy

$$\mathcal{E} \;\simeq\; 0.035\,\theta\,\psi_0^{3/2}\,B_0^{1/2} \quad , \tag{22}$$

almost independant of its configuration. This is the total energetic cost of completely detatching each pole from the background and connecting their fluxes together.

In three dimensions magnetic reconnection occurs along a field line called the separator (Greene 1988, Lau & Finn 1990, Longcope & Cowley 1996). The model predicts the morphology of the X-ray loop in terms of the configuration of the magnetic bipole. The length of the separator, projected onto the solar surface, is comparable to, but slightly larger than, the pole separation d, as given by eq. (19).

The separator is oriented along a direction intermediate between the bipole and the background field. The difference between bipole axis and separator axis, $\Delta\phi$ or $\Delta\phi'$, can be quantified in terms of parameters of the bipole.

6.2. Discussion

The mutual interaction of two magnetic poles is the simplest possible scenario in which reconnection can occur. An overlying field is necessary in order for there to be something to reconnect from. We have presented a model completely characterizing this scenario. The model retains only the basic elements necessary for this simplest case: point source poles, uniform background field, almost current-free corona (the minimum current corona). Each of these assumptions may be relaxed to yield a more complex model capable of more accurately representing particular events.

This work has considered only bipoles with matched fluxes: $\psi_+ = \psi_- = \psi_0$. If emergence is the manifestation of an arched flux tube (Ω-loop) encountering the solar surface, then we would expect the resulting poles to be matched. In the case of cancellation, however, the poles encounter one another by chance and there is no reason to expect them to have equal fluxes. Such a mismatched cancelation would leave behind a single pole with flux $|\psi_+ - \psi_-|$. Presumably the cancelled portion would be subducted, altough this would require dividing up the flux originally in the larger tube (Ryutova et al. 1997).

For the case of cancellation we should therefore generalize the model above to include $\psi_+ \neq \psi_-$. The characteristic flux, defined $\psi_0 \equiv \max(\psi_+, \psi_-)$, could be used to non-dimensionalize the problem as before. The bipole would be characterized by $\boldsymbol{\rho}$ as well as a new dimensionless variable

$$\xi \equiv \frac{\psi_+ - \psi_-}{\psi_0} \quad ,$$

within the range $-1 < \xi < 1$. This work has explored only the special case $\xi = 0$. In future work we will find $\hat{\psi}^{(\mathrm{v})}(\boldsymbol{\rho}, \xi)$, $\mathbf{F}(\boldsymbol{\rho}, \xi)$ and $\Delta\rho_0(\boldsymbol{\rho}, \xi)$ for values of $\xi \neq 0$. We expect ξ to remain fixed during the evolution of any bipole; only $\boldsymbol{\rho}$ can change in time.

The stick-slip model is a crude way of parameterizing ignorance of magnetic reconnection. Originally proposed by Longcope (1996) it is motivated by the number of possible mechanisms of fast reconnection which are triggered by instabilities. Each instability has a threshold which is related to total current either directly or indirectly. In fact, it has more basis in observation than in plasma physics. Those events attributed to magnetic reconnection, such as solar flares, or XBPs, release a certain amount of stored magnetic energy. If fast magnetic reconnection occurred under all circumstances (say $\theta = 0$) then no energy could ever be stored, and there would be no power associated with reconnection ($\bar{\mathcal{P}} = 0$). Perhaps the biggest puzzle posed by observations of magnetic reconnection is that it occurs sporadically. The stick-slip reconnection model is meant to reflect this fact.

The energy stored prior to reconnection is simply a function of the self-inductance of the current paths involved. If we look for the state with the *least* stored energy we find magnetic equilibria with singular currents along the separators (Longcope & Cowley 1996). While such a singular state will not occur in reality, it is a well defined lower bound on the stored energy. The self-inductance of the separator is simply its length, and this would not be much different in more sophisticated MHD treatments. Thus the energetic quantities found in this work essentially follow from simple dimensional arguments.

Questions about the time evolution of an X-ray bright point will be treated in future work, they cannot be self-consistently addressed using the quasi-static formalism of the MCC model. One result of a such a study, however, might be anticipated in advance. If the reconnection process, occurring at the separator itself, heats the plasma on loops passing through it, then these loops will fill with plasma and cool by radiation *after* they have crossed the separator. This introduces an asymmetry between the divergence and convergence scenarios, which is not strictly part of MCC. During convergence magnetic flux is crossing σ on its way into the P–N domain (the bipole); in the case of divergence the post-reconnection flux joins P–∞ and ∞–N. It seems less likely that energy deposited into large, open-ended loops, such as P–∞ or ∞–N, would result in chromospheric evaporation and X-ray emission. For this reason we expect that a more careful treatment will reveal that X-ray emission from small loops (i.e. XBPs) occur only during the process of convergence (cancellation). There is observational evidence supporting this kind of prediction (Webb et al. 1993).

The bipole reconnection model makes quantitative predictions in good agreement with typical observed values. Consider the parameters $\psi_0 = 10^{19}$ Mx, $B_0 = 10$ G and $v = 300\,\mathrm{m/sec}$, typical of bipoles accompanying XBPs. These lead to an interaction distance $d \leq 10$ Mm, comparable to observed values of both polar separations and XBP loop lengths. Bipoles which lack XBPs might correspond to poles outside their interaction distance. Alternatively, they might be interacting poles which are caught during a time between impulsive heating events. The expected fraction of such "latent" XBPs depends on the cooling time τ_{cool}. The life-time $t_{\mathrm{life}} = 5$ hours, is close to that inferred from XBP observations (Golub et al. 1974).

The predicted heating power, $\bar{\mathcal{P}} = 3\times 10^{23}\,\theta\,\mathrm{erg/sec}$, is less that values calculated by Kankelborg et al. (1997) for any choice of threshold in the expected regime $\theta \le 1$. The median observed value, $10^{24}\,\mathrm{erg/sec}$ can be obtained, however, with slightly adjusted parameters, such as $\psi_0 = 3\times 10^{19}$ Mx, $B_0 = 20$ G, $v = 500\,\mathrm{m/sec}$ and $\theta = 0.3$. The XBP survey of Kankelborg et al. does not measure these parameters, so it is difficult to establish the appropriate values.

The model has been presented using several simple parameters to facilitate more detailed observational comparison. The literature contains several observational XBP survey, but unfortunately none include all of the parameters required by the model. A new survey can be undertaken to identify XBPs and associated magnetic bipoles, measuring the parameters ψ_0, d and the flux mismatch ξ. The overlying magnetic field $\mathbf{B}_0$ can be determined from a large-scale model of the coronal field made using a full-disk magnetogram (Altschuler & Newkirk 1969). From all of these measured parameters the model will predict size, orientation of the XBP loop, and the radiated power $\bar{\mathcal{P}}$. These can be compared to measured values to test the reconnecting bipole model. A survey of bipoles and XBPs can be used to test the model statistically. This could be used to determine, observationally, the threshold parameter θ, providing insight into the process of magnetic reconnection as it occurs on the Sun.

The most difficult parameter to determine will be the background (overlying) magnetic field $\mathbf{B}_0$. The theoretical analysis in this work, however, clearly indicates what a critical role it plays in bipole reconnection. It is possible to derive relationships from which B_0 has been eliminated. For instance, using the fact that $d \sim \psi_0^{1/2}\,B_0^{-1/2}$ once the poles have begun to interact, it is possible to write

$$\bar{\mathcal{P}} \simeq 0.1\,\theta\,v\,\psi_0^2\,d^{-2} \quad . \tag{23}$$

This expression provides an alternative to the estimation of the large-scale field.

The foregoing work presents a model for magneetic reconnection between discrete magnetic features. It has been presented as a model for XBPs, but the same picture would apply to any pair-wise reconnection process. Recent studies have shown the photospheric magnetic field to be undergoing continuous emergence, fragmentation and cancellation (Schrijver et al. 1997). According to the model above, each pair-wise cancellation event should release an energy $\Delta\mathcal{E}$. With knowledge of the size distribution and cancellation rates, now available, it should be possible to estimate the net power dissipated through these events.

We thank Dr. C. C. Kankelborg for many helpful discussions on X-ray bright points, and for comments on the manuscript. This work was supported in part by NASA Grant NAG5–5043. This material is based upon work supported by the National Science Foundation under Grant No. ATM-9733424.

References

Altschuler, M. D., & Newkirk, G. 1969, Solar Phys., 9, 131

Baum, P. J., & Bratenahl, A. 1980, Solar Phys., 67, 245

Cargill, P. J. 1994, ApJ, 422, 381

Falconer, D. A., Moore, R. L., & Porter, J. G. 1997, in Proceedings of the High Resolution Solar atmospheric Dynamics Workshop, ed. E. E. DeLuca & J. Bookbinder

Golub, L., Krieger, A. S., Harvey, J. W., & Vaiana, G. S. 1977, Solar Phys., 53, 111

Golub, L., Krieger, A. S., Silk, J. K., Timothy, A. F., & Vaiana, G. S. 1974, ApJ, 189, L93

Gorbachev, V. S., & Somov, B. V. 1988, Solar Phys., 117, 77

Greene, J. M. 1988, JGR, 93, 8583

Habbal, S. R., Dowdy, J., J. F., & Withbroe, G. L. 1990, ApJ, 352, 333

Habbal, S. R., Ronan, R. S., Withbroe, G. L., Shevgaonkar, R. K., & Kundu, M. R. 1986, ApJ, 306, 740

Harvey, K. L., Nitta, N., Strong, K. T., & Tsuneta, S. 1994a, in X-ray solar physics from Yohkoh, ed. Y. Uchida, T. Watanabe, K. Shibata, & H. S. Hudson (Universal Academy Press), 21

Harvey, K. L., Strong, K. T., Nitta, N., & Tsuneta, S. 1994b, in Solar active region evolution: Comparing models with observations, ed. K. S. Balasubramaniam & G. W. Simon (A.S.P.), 377

Heyvarts, J., Priest, E. R., & Rust, D. M. 1977, ApJ, 216, 123

Kankelborg, C. C., Walker, A. B. C., II, & Hoover, R. B. 1997, ApJ, To appear Dec. 20

Kankelborg, C. C., Walker, A. B. C., II, Hoover, R. B., & Barbee, J., T. W. 1996, ApJ, 466, 529

Lau, Y.-T., & Finn, J. M. 1990, ApJ, 350, 672

Longcope, D. W. 1996, Solar Phys., 169, 91

Longcope, D. W., & Cowley, S. C. 1996, Phys. Plasmas, 3, 2885

Longcope, D. W., & Fisher, G. H. 1996, ApJ, 458, 380

Longcope, D. W., & Strauss, H. R. 1994, ApJ, 437, 851

Mandrini, C. H., Démoulin, P., Van Driel Gesztelyi, L., Schmieder, B., Cauzzi, G., & Hafmann, A. 1996, Solar Phys., 168, 115

Marion, J. B., & Thornton, S. T. 1988, Classical Dynamics of Particles and Systems (third ed.) (Harcourt Brace Jovanovich, San Diego)

Nolte, J. R., Solodyna, C. V., & Gerassimenko, M. 1979, Solar Phys., 63, 113

Parnell, C. E., Priest, E. R., & Golub, L. 1994, Solar Phys., 151, 57

Priest, E. R., & Démoulin, P. 1995, JGR, 100, 23,443

Priest, E. R., & Milne, A. M. 1980, Solar Phys., 65, 315

Priest, E. R., Parnell, C. E., & Martin, S. F. 1994, ApJ, 427, 459

Ryutova, M., Schrijver, C. J., Shine, R. A., Tarbell, T., Berger, T., & Title, A. M. 1997, in Proceedings of the High Resolution Solar Atmospheric Dynamics Workshop, ed. E. E. DeLuca & J. Bookbinder

Schrijver, C. J., Title, A. M., Van Ballegooijen, A. A., Hagenaar, H. J., & Shine, R. A. 1997, ApJ, 487, 424

Somov, B. V. 1992, Physical Processes in Solar Flares (Kluwer)

Strong, K. T., Harvey, K., Hirayama, T., Nitta, N., Shimizu, T., & Tsuneta, S. 1992, PASJ, 44, L161

Syrovatskii, S. I. 1981, ARA&A, 19, 163

Webb, D. F., Martin, S. F., Moses, J. W., & Harvey, J. W. 1993, Solar Phys., 144, 15